Moment Gradient Factor for Lateral–Torsional Buckling of T-Shaped Beams

Michael Manarin[1], Robert G. Driver[2], Yong Li[3]

Abstract

Lateral–torsional buckling (LTB) is a potential limit state for steel beams. Particularly, T-shaped beams (referred to as beams with WT-sections) can be sensitive to this failure mode due to the presence of only a single flange. Current LTB capacity equations in both CSA Standard S16 and AISC 360 neglect the moment gradient effect by prescribing a moment gradient factor of 1.0 when determining the critical moment for T-shaped beams. This study aims to assess the adequacy of the current moment gradient factor (1.0) for LTB capacity of simply supported T-shaped beams through numerical studies. The elastic critical moments of thirteen representative T-shaped beams subjected to a constant moment, a point load, or a uniformly distributed load are determined numerically using LTBeam and ABAQUS, a free and commercial software, respectively. Numerical analyses using both tools led to the finding that the elastic critical moments of T-shaped beams are affected by moment distributions. This study implies that T-shaped beams should have approximately the same moment gradient factor as I-shaped beams when subjected to single-curvature loading. Further work is required to assess the adequacy of the current moment gradient factor (1.0) in predicting the inelastic critical moments for LTB of simply supported T-shaped beams.

1. Introduction

Lateral–torsional buckling (LTB) is a potential limit state for beams where the member deflects laterally and twists between brace points in a coupled stability failure. The LTB design equations in both CSA Standard S16, *Design of Steel Structures*, and AISC 360, *Specification for Structural Steel Buildings*, utilize a moment gradient factor, ω_3 or C_b, respectively, to account for varying moments along the beam length. The moment gradient factors for doubly-symmetric beams have been well studied. For example, equations for moment gradient factors to account for linear moment distributions with unequal end moments (Salvadori 1955) is accepted in both the CSA S16 (2014) and AISC 360 (2016), while general moment distributions proposed by Kirby and Nethercot (1979) and Wong and Driver (2010) are both accepted in the AISC 360 (2016) and the latter is also accepted in the CSA S16 (2014). The authors are aware of a pre-publication paper that claims the equation for the moment gradient factor initially proposed by Wong and Driver (2010) for doubly-symmetric, I-shaped beams is valid for singly-symmetric I-shaped beams in

---

[1] M.Sc. Candidate, University of Alberta, <manarin@ualberta.ca>
[2] Professor, University of Alberta, <rdriver@ualberta.ca>
[3] Assistant Professor, University of Alberta, <yong9@ualberta.ca>

single curvature and can be modified slightly for singly-symmetric I-shaped beams in reverse curvature.

T-shaped beams can be particularly sensitive to LTB failure due to the presence of only a single flange. The LTB design equations in both CSA Standard S16 and AISC 360, neglect the moment gradient effect by using a moment gradient factor, $\omega_3 = 1$ or $C_b = 1$, when determining the critical moment for T-shaped beams. For consistency, the remainder of this paper will utilize C_b to represent the moment gradient factor (CSA 2014, American Institute of Steel Construction 2016) for T-shaped beams, also referred to as beams with WT-sections. This inherently conveys that WT-sections do not abide by the same LTB principles as W-sections and singly symmetric I-shaped sections because these moment gradient factors use a quarter point method, as shown in Eq. 1,

$$C_b = \frac{4M_{max}}{\sqrt{M_{max}^2 + 4M_a^2 + 7M_b^2 + 4M_c^2}} \tag{1}$$

where M_a, M_b and M_c are the moments at one-quarter, half and three-quarter points of the beam segment, respectively, and M_{max} is the maximum moment along the beam segment. This equation is accepted both in the AISC 360 (2016) and the CSA S16 (2014).

Concerns regarding T-shaped beams were initially determined using the energy approach (Kitipornchai and Wang 1986). The analysis focused on linear moment gradients and reverse curvature results; however, to the best of the authors' knowledge, little effort attempted to address the moment gradient factor for T-shaped beams. This research aims to assess the adequacy of the current moment gradient factor ($C_b = 1$) in predicting the elastic critical moments for LTB capacity of simply supported T-shaped beams through numerical studies. The elastic critical moments of thirteen representative T-shaped beams, subjected to a constant moment, a point load, or a uniformly distributed load (UDL), are determined numerically using LTBeam and ABAQUS, a free and commercial software, respectively. Accordingly, the moment gradient factors for the load scenarios with moment gradient (e.g., a point load, and a UDL) are calculated and reported.

2. Test Matrix for Numerical Analyses
This study considers simply supported T-shaped beams with varying lengths. The WT-sections are selected from the 283 WT-sections available in the AISC online Shapes Database (AISC 2017) which includes shapes not in the CISC Handbook of Steel Construction (CISC 2017). Of the 283 WT-sections, 178 sections are considered susceptible to the failure mode of LTB considering the second moment of area about the strong axis (I_x) must be greater than the second moment of area about the weak axis (I_y). The sections susceptible to LTB vary in depth from 100 to 560mm (4 to 22 inches) and 100 to 470mm (4 to 18.5 inches) in width. The web thickness and flange thickness varies from 4 to 77mm (0.15 to 3 inches) and 5 to 115mm (0.2 to 4.5 inches). To balance the computational cost with design space coverage in this study, representative WT-sections are selected based on section classes, top flange thickness and width, web thickness and depth, area moment of inertia, and minimum slenderness ratio for global elastic LTB. The minimum slenderness ratio is defined as the ratio between the minimum beam length (L) for the T-shaped beams susceptible to elastic LTB and the section depth (h).

2

The section candidates susceptible to LTB are first grouped into class 1, 2, and 3 sections based on the classification criteria for elements in flexural compression using a yield stress of 345 MPa (CSA S16 2014). Since the flange is in compression and the web is in tension, the section class is determined based on the flange class. There are 162 class 1 sections, thirteen class 2 sections, three class 3 sections. Class 4 sections are not considered within this study due to their limited use. A subset of each class is selected to cover the range of section properties and minimum slenderness ratio for global elastic LTB. Figures 1 - 4 show all the section candidates (denoted as open markers) and the sections selected (denoted as closed markers) with section classes differentiated by shapes. These plots indicate the selected sections have good coverage of top flange width and thickness, web depth and thickness, second moments of area I_x and I_y, minimum slenderness ratio for global elastic LTB and section depth.
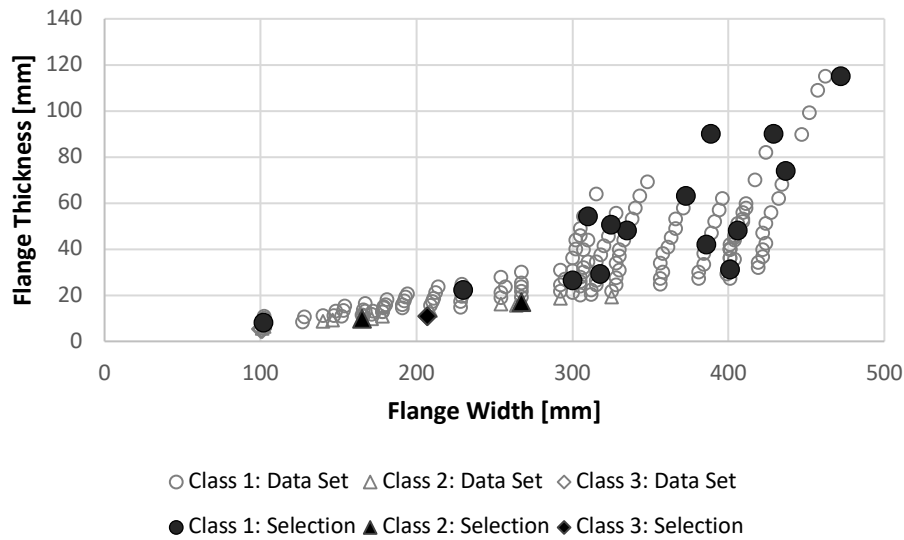

Figure 1: Section Candidates vs Sections Selected: Top Flange
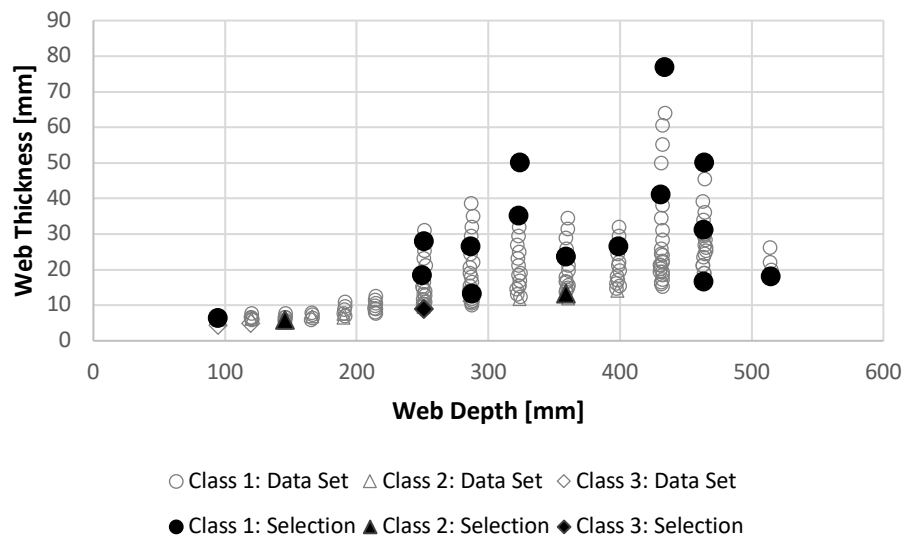

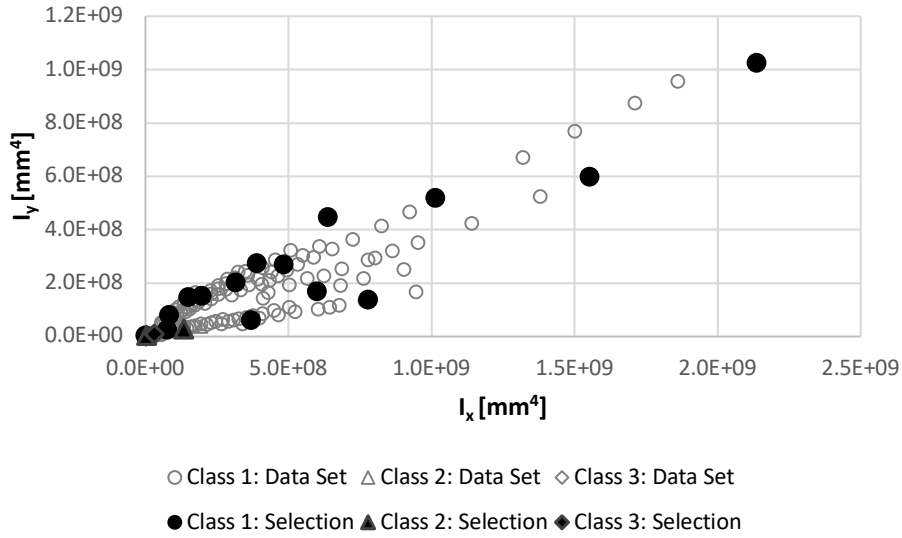Figure 2: Section Candidates vs Sections Selected: Web

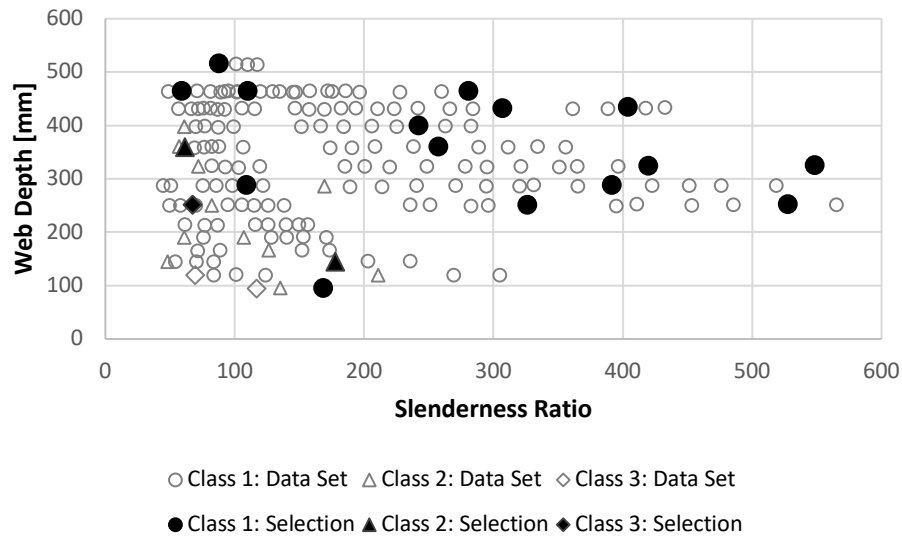Figure 3: Section Candidates vs Sections Selected: Second Moment of Area

Figure 4: Section Candidates vs Sections Selected: Minimum Slenderness Ratio for Global Elastic LTB

Note that the beams considered in this study are not practical as indicated by the minimum slenderness ratios, which are extremely large, to be susceptible to global elastic LTB. For example, the beam with a WT380x194.5 section needs to have a global slenderness ratio of approximately 200 (i.e., 78 m long) to be susceptible to elastic LTB. The authors acknowledge that the beams studied are not practical, as T-shaped beams with economical lengths will likely fail in inelastic LTB, instead of elastic LTB. However, this study aims to serve the basis to determine the inelastic critical moment, as the elastic critical moment is commonly used to calculate the inelastic critical moment in design equations (CSA 2014).

4

3. Numerical Analyses Tools and Model Validation

The moment gradient factor in both CSA S16 and AISC 360 derives from the study of simply supported beams with fork supports at both ends (see Fig. 5), i.e., lateral translation (U1) constrained, vertical translation (U2) constrained, and twist (UR3) constrained (Ziemian 2010). The longitudinal translation (U3) is constrained at the right end, but free at the left end of the simply supported beam. Accordingly, elastic critical moments of steel beams subjected to a constant moment, a point load, or a UDL are determined and used to determine the moment gradient factor, which aims to account for the effects of moment variation along the beam length on the LTB capacity. In this study, the elastic material properties for steel considered are the modulus of elasticity, E = 200 GPA and the Poisson's ratio, $v = 0.3$.
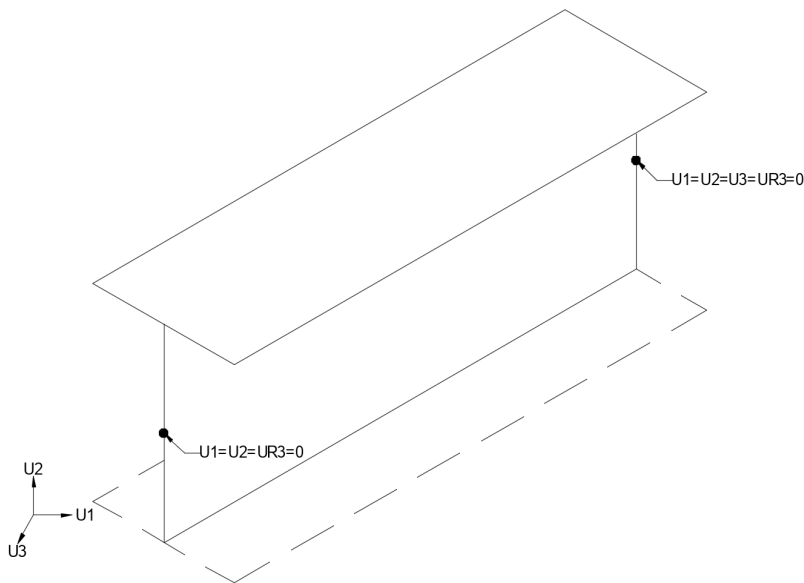

Figure 5: Schematic View of the Simply Supported Beam Studied with Fork Supports (i.e., Flexurally Pinned Boundary Conditions) for LTB Analysis

Two different tools (i.e., LTBeam and ABAQUS) are utilized to facilitate the numerical analysis. Due to the lack of experimental data, two programs, which utilize different methods to solve the LTB problem, are used to co-validate the elastic critical moments. Their applications to predicting the LTB capacity are briefly explained as follows.

3.1 LTBeam

LTBeam, is a freely available software (Centre Technique Industriel de la Constrution Metallique 2001), that is used to calculate the elastic critical moment by solving the classic eigenvalue problem using an iterative dichotomic process without considering initial imperfections. This tool has been validated by other analysis tools (e.g., commercial finite element software, ANSYS). For example, the maximum difference is only 1.48% between LTBeam and ANSYS in predicting the elastic critical moments for six T-shaped beams (Centre Technique Industriel de la Constrution Metallique 2002). As such, LTBeam can be used to predict the elastic critical moment, as stated in the Non-contradictory, Complementary Information (NCCI) portion of the Eurocode (Bureau 2008).

3.2 ABAQUS

5

LTB analysis using the commercial finite element software ABAQUS (Dassault Systèmes 2018) can be performed through eigenvalue analysis without considering the initial geometric imperfection as LTBeam does, or through nonlinear static analysis (i.e., riks), which is more challenging and time-consuming. However, the riks approach allows the incorporation of initial imperfection (e.g., geometrical imperfection and residual stress) and the characterization of the equilibrium path. In order the predict the LTB capacity, a buckling analysis, also known as an eigenvalue analysis, is first performed to determine the elastic critical moments, which are found to be significantly close to the LTB analysis, and to verify the finite element model to a certain degree. Additionally, the eigen-buckling modes from eigenvalue analysis facilitate the approximation of initial geometric imperfection. An initial imperfection (length/1500) is imposed on the beam based on the first eigen-buckling mode, and a static riks analysis is followed to determine the elastic critical load.

Unlike the pre-defined boundary conditions in LTBeam, the implementation of the corresponding boundary conditions in the finite element model is by no means trivial. The finite element model typically requires validation by correlation studies between numerical with experimental predictions. In this study, the finite element model is validated using experimental results for doubly-symmetric I-shaped beams, and then used for T-shaped beams due to lack of corresponding experimental data.

The boundary conditions shown in Fig. 5 are implemented as illustrated in Fig. 6. There are two types of constraints that can be used within ABAQUS to model the end restraints: rigid body ties and kinematic coupling. A rigid body tie forces the slave nodes to move with the master node as a rigid body. The kinematic coupling is different from rigid body ties in that the element still moves as a rigid body, but only for the coupled degrees-of-freedom (DOFs) selected by the user. Referring to Fig. 6, all the translational and rotational DOFs are kinematically coupled except U3, the longitudinal direction.
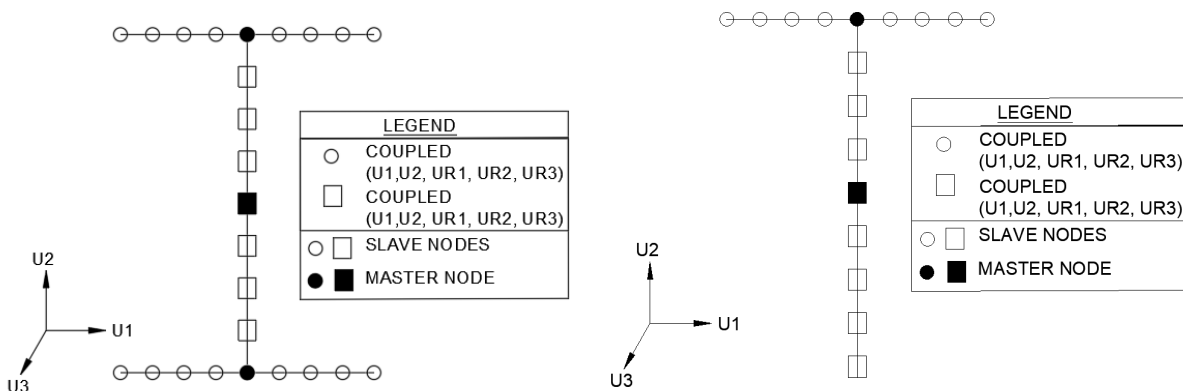

Figure 6: Boundary conditions; I-shape (left), T-shape (right)

The finite element modeling strategy is validated using the lateral–torsional buckling tests of I-shaped beams from Nagoya University (Fukumoto et al. 1980). Twenty-five beams were tested for each length—2.6m, 2.0m and 1.5m—and one set of the load-deflection curves for beams of three different lengths but the same section was reported and used for validation in this study. This set of load-deflection curves—excluding the initial geometric imperfection in the deflection values—is for doubly-symmetric I-shaped beams with the dimensions of the cross-section as

6

200mm (web height) x 100mm (flange width) x 5.5mm (web thickness) x 8mm (flange thickness). The material properties were obtained from coupon tests: the modulus of elasticity is 201.7 GPa, the yield stress of the flange plates is 252 MPa, and the yield strength of the web plate is 287 MPa. Note that realistic residual stress is also included according the experimental data reported.
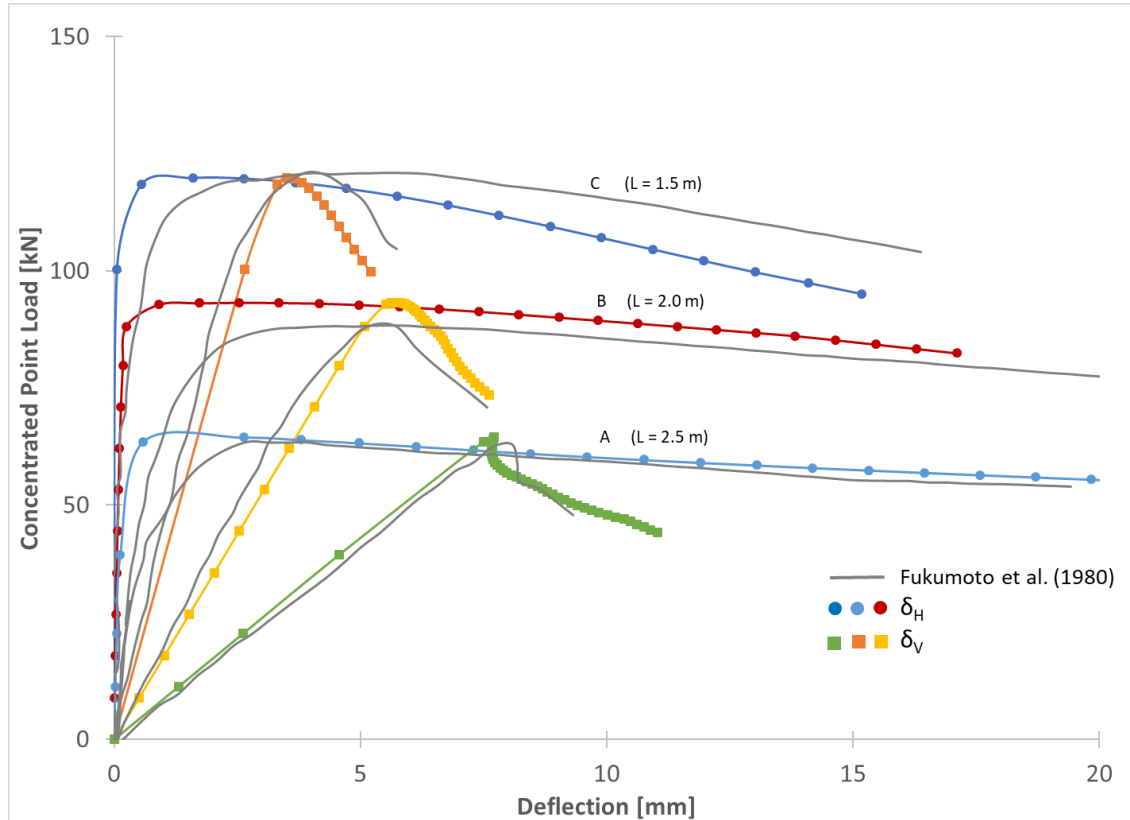

Figure 7: Model Verification

Figure 7 shows the comparison of the load-deflection curves obtained from the finite element models and the tests, where δ_H is the horizontal deflection of the extreme fibre of the top flange, and δ_V is the vertical deflection of the centre of the bottom flange at the mid-span of the beam. The comparison displays a reasonably good correlation between the numerical prediction and experiment measurements with due consideration of the challenges (e.g., incomplete information, and unknown measurement error). The initial stiffness is either slightly over-estimated or under-estimated; this may be due to the initial geometric imperfection assumed. The initial imperfection was reported as less than length/5000 without information on the imperfection distribution along the beam. In the numerical analysis, an initial imperfection is thus assumed to take the same shape as the first eigen-buckling mode with a maximum lateral displacement of length/5000. Overall, the model can reasonably predict the LTB behaviour of doubly symmetric I-shaped beams, and thus a similar model can be used to predict the LTB behaviour of T-shaped beams as studied in this work. The same boundary conditions as defined earlier are used in the numerical analysis of T-shaped beams under a point load and a UDL, except under a constant moment condition. The constant moment loading is realized by applying point loads at tips of the flange and web, and at both ends of the beam. As such, a minor modification was made to the boundary conditions for the beam,

i.e., coupling U3 for all nodes along the web, to avoid numerical issues caused by extreme distortion of the web locally without affecting the global behaviour.

4. LTB Analysis Results

The moment gradient factor, C_b, is determined by comparing the elastic critical moments of a beam subject to a varying moment condition (e.g., a point load or a UDL) with that subject to a constant moment condition. To be specific, C_b for a point load condition is calculated as the ratio between the elastic critical moment of a beam under a point load and that under a constant moment. Similarly, C_b for a UDL can be calculated. This leads to a critical moment multiplier or the moment gradient factor, C_b, to account for the effect of moment variation along the beam on the critical moment readily in the design process. Using the formula by Wong and Driver (2010), see Eq. 1, the moment gradient factor is 1.265 for a point load condition and 1.13 for a UDL condition,. These two values will be used as reference values of C_b for the purpose of comparison.

4.1 Eigenvalue analysis results

The elastic critical moments determined using LTBeam are utilized to calculate the moment gradient factors as reported in Table 1.

Table 1: Moment gradient factor based on eigenvalue analysis in LTBeam

Section	C_b Constant Moment	C_b Point Load	C_b UDL
WT460X688.5	1.000	1.352	1.129
WT345X401	1.000	1.351	1.129
WT500X247	1.000	1.365	1.136
WT500X488	1.000	1.355	1.130
WT100X11.25	1.000	1.378	1.145
WT420X236.5	1.000	1.362	1.135
WT380X194.5	1.000	1.364	1.136
WT345X274	1.000	1.354	1.130
WT305X186	1.000	1.356	1.131
WT265X109.5	1.000	1.365	1.136
WT265X184.5	1.000	1.354	1.130
WT460X393.5	1.000	1.356	1.131
WT550X171	1.000	1.393	1.155
WT305X70	1.000	1.380	1.146
WT500X124	1.000	1.393	1.156
WT380X73	1.000	1.401	1.163
WT155X19	1.000	1.392	1.153
WT265X36	1.000	1.408	1.169
Average		1.371	1.141
Standard Dev.		0.019	0.013

Table 1 shows the C_b values are tightly grouped with very small standard deviations for both loading scenarios. The C_b value for a point load is larger than the value obtained using Eq. 1. Note

8

that prior to using the quarter-point formulas, C_b values were tabulated for a select number of loading scenarios and $C_b = 1.371$ for point loads (Nethercot and Trahair 1976). Additionally, $C_b = 1.141$ for a UDL, which is approximately the same as Eq. 1. However, the geometric imperfection is not considered here, which will be addressed in the riks-based LTB analysis.

4.2 Riks-based LTB analysis results
The riks analysis in ABAQUS provides the load-deflection curve, e.g., the load versus the lateral deflection at the middle height of the web at the midspan of the beam. See Fig. 8 for the load-deflection curve for the beam that has a WT420x236 section and a slenderness ratio (length/height) of 185. The load-deflection curve, which is usually employed to determine the elastic critical moment, behaves nonlinearly due to the initial geometric imperfection and the nonlinear geometric stiffness. The slope of the load-deflection curve is an equivalent (generalized) stiffness to resist LTB. For example, if the load-deflection curve starts to soften, the capability to resist LTB starts to degrade. A common practice is to define the critical load corresponding to zero slope, and the maximum associated moment in the vertical plane is regarded as the critical moment. C_b is determined for the point load and UDL scenarios using the moments obtained from riks analysis in ABAQUS.

In Fig. 8, the load-deflection curves are plotted in Fig. 8(a), (b) and (c) for the load scenarios of a constant moment, a point load, and a UDL, respectively; the moment-deflection curves for these three load scenarios are shown in Fig. 8(d). Note that the vertical axis in Fig. 8(a) is the constant moment, while in Fig. 8(b) and (c) the vertical axes are the total load applied. The moment in Fig. 8(d) is the maximum moment at the midspan of the beam. The three loading scenarios are included in Fig. 8(d) to identify the effect of the loading scenario. Figure 8 does not include the initial imperfections in the lateral displacement. The inclusion of imperfections would increase the lateral displacement an additional 55mm. Although this accounts for approximately 10% of the lateral displacement at the critical state for this section, it can account for over 50% of the displacement in some of the sections studied.
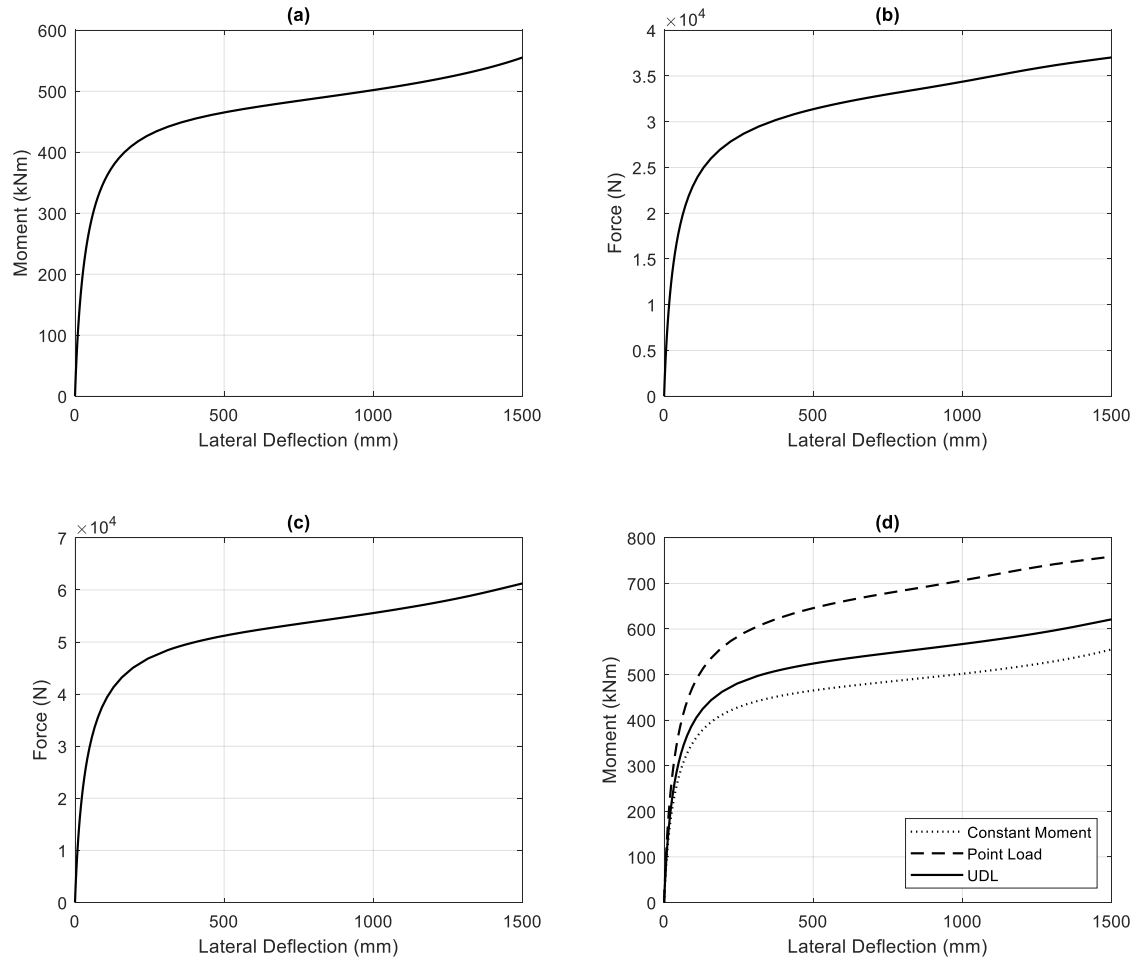
9

Figure 8: Load Deflection Curves for Beams with a WT420x236 Section: (a) Constant Moment; (b) Point Load; (c) UDL; and (d) Moment Deflection Curves for all Three Loading Scenarios.

When analyzing the load-displacement curves for the beams considered, it is found that the slope of the load-deflection curves rarely approach zero (e.g., 100% stiffness loss) even with a large deflection (e.g., 18% of the length). In this study, a significant stiffness loss (i.e., 95%) compared with the initial stiffness is considered as a critical state, since these load-displacement curves do not all obtain a slope of zero. To determine the critical moment, the lateral deflection at the critical load is recorded and the corresponding moment at the recorded lateral deflection is the associated critical moment.

A few beams also show a so-called snap-back behaviour in the load-deflection curve, i.e., the deflection starts to decrease with the increase of load after a certain deflection. For this case, the turning point is taken as a critical point if the significant stiffness loss has not been reached. The critical points are automatically determined following the above algorithm for all beams, except one out of 39 cases considered in this study. For the beam with a WT305x186 section, and subjected to a point load, it is found that this beam suffers a 95% stiffness loss when the associated moment is equal to 49% (or 46%) of the critical moment for the constant moment (or UDL) condition. However, it is believed that the critical moment corresponding to a point load condition should be at least as large as that for the constant moment or UDL condition. Thus, the critical

10

point in this case is chosen as the point such that the critical moment of the T-beam under a point load, is equal to that under the constant moment condition.

The slow stiffness softening and even stiffness hardening, in some beams (e.g., a WT345x274 section) with a snap-back, happen to these non-practical beams with large slenderness ratios (e.g., 315) and lengths (e.g., 120m). It is suspected that the analysis detects another equilibrium path at the snap-back point and diverts to the so-called "new" equilibrium path which needs to be confirmed using more advanced algorithms.

The moment gradient factors based on the riks analysis in ABAQUS are presented in Table 2. The moment gradient factor is 1.395 and 1.181 for a point load and a UDL, respectively. As previously stated, the reference values from CSA S16 are 1.265 and 1.13. Thus, C_b for a point load scenario is 10.3% larger, and C_b for a UDL scenario is 4.5% larger than the values prescribed by CSA S16.

Table 2: Moment gradient factors based on riks analysis in ABAQUS

Section	C_b for Constant Moment	C_b for Point Load	C_b for UDL
WT460X688	1.000	1.424	1.097
WT345X401	1.000	1.415	1.007
WT500X247	1.000	1.521	1.285
WT500X488	1.000	1.421	1.123
WT100X11	1.000	1.379	1.198
WT420X236	1.000	1.369	1.182
WT380X194	1.000	1.438	1.178
WT345X274	1.000	1.462	1.163
WT305X186	1.000	1.000	1.073
WT265X109	1.000	1.125	1.072
WT265X184	1.000	1.122	1.047
WT460X393	1.000	1.515	1.184
WT550X171	1.000	1.555	1.226
WT305X70	1.000	1.473	1.245
WT500X124	1.000	1.544	1.377
WT380X73	1.000	1.557	1.330
WT155X19	1.000	1.184	1.078
WT265X36	1.000	1.610	1.397
Average		1.395	1.181
Standard Dev.		0.174	0.113

4.3 Discussion

11

There is a larger dispersion in C_b obtained from the riks analysis in ABAQUS when compared to C_b from eigenvalue analysis in LTBeam. This is partly due to the initial geometric imperfection considered and the algorithm used in this paper to determine the critical point and thus the elastic critical moment. Eigenvalue analysis in LTBeam determines the elastic critical moment using the system of equations from the first principles of buckling. Due to the mathematical nature, the results are not influenced by other factors. The riks analysis in ABAQUS uses an equilibrium path to determine the elastic critical moment of the beam, in which the effect of initial geometric imperfection is considered.

The results from eigenvalue analysis and riks analysis both confirm that the moment gradient for T-shaped beams has similar effects as indicated by C_b to I-shaped beams. The beams analyzed would be uneconomic to be used in practice as they are overly slender; however, the elastic critical moment is required to calculate the inelastic LTB moment in the design process. Further studies need to be performed to evaluate the adequacy of Eq. 1 or to develop a new equation for C_b. This will be used to determine the inelastic critical moment of T-shaped beams.

5. Conclusion

The moment gradient factor, $C_b = 1$, tends to be overly conservative for T-shaped beams susceptible to elastic lateral–torsional buckling in the CSA S16 and AISC 360. It is observed that the moment gradient factors for T-shaped beams depend on the moment distribution and are comparable to the moment gradient factors for doubly-symmetric and singly-symmetric I-shaped beams. The preliminary study presented here shows that $C_b = 1.395$ for a point load at the midspan and 1.181for uniformly distributed loading. Further research is required to determine if Eq. 1 is applicable to T-shaped beams. Research is currently underway to determine the inelastic critical moment when the beam fails in inelastic lateral–torsional buckling under three loading scenarios: a constant moment, a point load at midspan, and a uniformly distributed load.

Acknowledgments

References

AISC. (2017). "AISC Shapes Database v15.0". Available from https://www.aisc.org/globalassets/aisc/manual/v15.0-shapes-database/aisc-shapes-database-v15.0.xlsx.

American Institute of Steel Construction. (2016). "Specification for Structural Steel Buildings, ANSI / AISC 360-16". AISC, Chicago.

Bureau, A. (2008). "NCCI: Elastic Critical Moment for Lateral Torsional Buckling".

Centre Technique Industriel de la Construction Metallique. (2001). "LTBeam".

Centre Technique Industriel de la Construction Metallique. (2002). "LTBeam Report on Validation Tests". (July) 1–21.

CISC. (2017). "Handbook of Steel Construction". *In* 11th ed. Canadian Institute of Steel Construction, Toronto, ON.

CSA. (2014). "CSA S16: Design of Steel Structures". Canadian Standards Association, Toronto.

Dassault Systèmes. (2018). "ABAQUS". ABAQUS Inc.

Fukumoto, Y., Itoh, Y., and Kubo, M. (1980). "Strength Variation of Laterally Unsupported Beams". *Journal of the Structural Division, ASCE*, 106(ST1) 165–181.

Kirby, P.A., and Nethercot, D.A. (1979). "Design for Structural Stabilitiy". Halsted Press, New York, NY.

Kitipornchai, S., and Wang, C.M. (1986). "Lateral Buckling of Tee Beams Under Moment Gradient". *Computers and*

Structures, 23(1) 69–76.

Nethercot, D.A., and Trahair, N.S. (1976). "Lateral Buckling Approximations for Elastic Beams". *Structural Engineer*, 54(6) 197–204.

Salvadori, M.G. (1955). "Lateral Buckling of I-Beams". *ASCE Transactions*, 120 1165–1177.

Wong, E., and Driver, R.G. (2010). "Critical Evaluation of Equivalent Moment Factor Procedures for Laterally Unsupported Beams". *Engineering Journal*, 47(1) 1–20.

Ziemian, R.D. (2010). "Guide to Stability Design Criteria for Metal Structures". *In* 6th ed. John Wiley & Sons, Inc, New Jersey.